



Research article

A pseudospectral method for investigating the stability of linear population models with two physiological structures

Alessia Andò^{1,5}, Simone De Reggi^{2,5,*}, Davide Liessi^{2,5} and Francesca Scarabel^{3,4,5}

¹ Area of Mathematics, Gran Sasso Science Institute, viale F. Crispi 7, 67100 L'Aquila, Italy

² Department of Mathematics, Computer Science and Physics, University of Udine, via delle Scienze 206, 33100 Udine, Italy

³ Department of Mathematics, The University of Manchester, Oxford Rd, M13 9PL, Manchester, United Kingdom

⁴ Joint UNiversities Pandemic and Epidemiological Research, United Kingdom

⁵ CDLab – Computational Dynamics Laboratory, University of Udine, Italy

* **Correspondence:** Email: simone.dereggi@uniud.it.

Abstract: The asymptotic stability of the null equilibrium of a linear population model with two physiological structures formulated as a first-order hyperbolic PDE is determined by the spectrum of its infinitesimal generator. In this paper, we propose a general numerical method to approximate this spectrum. In particular, we first reformulate the problem in the space of absolutely continuous functions in the sense of Carathéodory, so that the domain of the corresponding infinitesimal generator is defined by trivial boundary conditions. Via bivariate collocation, we discretize the reformulated operator as a finite-dimensional matrix, which can be used to approximate the spectrum of the original infinitesimal generator. Finally, we provide test examples illustrating the converging behavior of the approximated eigenvalues and eigenfunctions, and its dependence on the regularity of the model coefficients.

Keywords: bivariate collocation; infinitesimal generator; partial differential equations; stability of equilibria; physiologically structured populations

1. Introduction

Mathematical models are often used to describe the evolution of populations in biology and epidemiology. An important class of models that has attracted increased attention is that of structured population models, in which individuals are characterized by one or more variables that describe the *i*-state (i.e., the individual state) and determine the individual processes, including for instance birth,

growth and death. Examples of physiological structures are age, size, spatial position or time since infection. We here focus on a class of structured population models where the structuring variables are continuous and the models are formulated as first-order hyperbolic partial differential equations (PDEs) (see, e.g., [1-5] and references therein). In particular, we consider the case where individuals are characterized by two different traits [6, 7].

In applications to population dynamics, the interest is often focused on the long-term properties of the systems, for instance the existence of equilibrium states and their stability. For linear models with two structures, it has been proved that the stability of the null equilibrium is determined by the spectrum of the infinitesimal generator (IG) of the semigroup of solution operators [8, 9]. Since the IG is an operator acting on an infinite-dimensional space of functions, numerical techniques are required to obtain finite-dimensional approximations of the operator and, in turn, of its spectrum.

For the analysis of local stability of equilibria, pseudospectral methods have been widely used both for delay equations [10-13] and for PDE population models with one structuring variable [14-16]. The main advantage of pseudospectral methods is their typical spectral accuracy, by which the order of convergence of the approximation error increases with the regularity of the approximated function. In particular, the convergence is exponential for analytic functions [17]. In the case of delay equations, this implies that the spectrum of the IG is approximated with exponential order of convergence, as the corresponding eigenfunctions are exponentials (see, e.g., [18, Proposition 3.4]). In the case of PDEs, the eigenfunctions are still exponential in time, but the order of regularity with respect to the physiological variables depends on the regularity of the model parameters, which therefore affects the order of convergence of the approximation [9, Theorem 3.2]. A similar behavior has been shown for the approximation of R_0 for structured epidemic models [19-21], and the approximation of the solution operators [22-24].

For structured models with one single structuring variable, pseudospectral methods have already been proposed to study the stability of the null equilibrium in [14]. In that paper the IG is approximated by combining pseudospectral differentiation with the inversion of a (linear) algebraic condition characterizing the domain of the operator. However, implementing this technique becomes substantially more involved in the presence of more structuring variables.

A different approach, which has been successfully employed in the context of nonlinear PDEs with one physiological variable [16] and of renewal equations [25, 26], consists in first reformulating the problem at hand via conjugation with an integral operator, and then approximating the resulting transformed operator via pseudospectral techniques. The advantages of this approach are mainly twofold: on the one hand, the transformed operator acts on a space of absolutely continuous functions (rather than the original space L^1), hence point evaluation, as well as polynomial interpolation and collocation, are well defined; on the other hand, the domain of the transformed operator is characterized by a trivial condition (specifically, a zero boundary condition), which substantially simplifies the numerical implementation. From a modeling point of view, the integrated state has a clear interpretation as it represents the number of individuals whose i -state is less than a given value.

Goal of this work is to introduce a numerical method for the stability analysis of linear PDE population models with two structuring variables based on this second approach. As far as we know, there is currently no other numerical method available for this problem. We demonstrate the applicability and computational efficiency of the new method with several numerical tests, illustrating the convergence of the approximated eigenvalues to the exact ones and supporting the conjecture of spectral accuracy,

and we apply the method to two interesting test problems from epidemiology and ecology.

The paper is organized as follows. In Section 2 we introduce the prototype model and the relevant solution operators and IG. Section 3 describes the reformulation of the IG in terms of the integrated state. The reformulated IG is discretized in Section 4 and the resulting numerical method is applied to some test problems in Section 5. In Section 6 we discuss the extension to models with structuring variables evolving with nontrivial velocities and show an example. In Section 7 we apply the method to an epidemiological model structured by age and time since infection [6] and to a population model structured by age and size [7]. Finally, we provide some concluding remarks in Section 8. In Appendix A, for completeness, we apply the method to the case of one structuring variable and illustrate it with a test model.

A MATLAB implementation of the method is available at <http://cdlab.uniud.it/software>.

2. The prototype model

Let $x_0, \bar{x}, y_0, \bar{y} \in \mathbb{R}$ such that $x_0 < \bar{x}$ and $y_0 < \bar{y}$ and let $\Omega := [x_0, \bar{x}] \times [y_0, \bar{y}]$. We consider the scalar first-order linear hyperbolic PDE

$$\partial_t u(t, x, y) + \partial_x u(t, x, y) + \partial_y u(t, x, y) = -\mu(x, y)u(t, x, y), \quad (2.1)$$

with boundary conditions

$$u(t, x, y_0) = \iint_{\Omega} \alpha(x, \xi, \sigma) u(t, \xi, \sigma) d\xi d\sigma =: K_{\alpha}(u(t, \cdot, \cdot))(x), \quad (2.2)$$

$$u(t, x_0, y) = \iint_{\Omega} \beta(y, \xi, \sigma) u(t, \xi, \sigma) d\xi d\sigma =: K_{\beta}(u(t, \cdot, \cdot))(y), \quad (2.3)$$

where $u(t, x, y)$ is the density of the given population at time $t \geq 0$ depending on the two structuring variables $x \in [x_0, \bar{x}]$ and $y \in [y_0, \bar{y}]$. Here, the rate $\mu(x, y)$ represents the per capita mortality rate of individuals in state (x, y) , while $\alpha(x, \xi, \sigma)$ and $\beta(y, \xi, \sigma)$ describe the per capita rates at which individuals in state (ξ, σ) produce new individuals in state (x, y_0) and (x_0, y) , respectively.

Following [8, Assumption 2.1], we assume that the model coefficients $\mu: \Omega \rightarrow \mathbb{R}$, $\alpha: [x_0, \bar{x}] \times \Omega \rightarrow \mathbb{R}$ and $\beta: [y_0, \bar{y}] \times \Omega \rightarrow \mathbb{R}$ are nonnegative functions, with μ an L^1_{loc} function* on $[x_0, \bar{x}] \times [y_0, \bar{y}]$, α and β L^1 functions, $\alpha(x, \cdot, \cdot)$ and $\beta(y, \cdot, \cdot)$ dominated by L^1 functions in x and y , respectively, and μ bounded away from 0 (for a similar but more general approach, see [27, Section 4]). Observe that the operators K_{α} and K_{β} map $L^1(\Omega)$ to $L^1([x_0, \bar{x}])$ and $L^1([y_0, \bar{y}])$, respectively, and are bounded.

Under these assumptions, for every $u_0 \in L^1(\Omega)$ the initial–boundary value problem defined by (2.1)–(2.3) and $u(0, \cdot, \cdot) = u_0$ admits a unique solution $u(t, \cdot, \cdot) \in L^1(\Omega)$ for $t \geq 0$. Moreover, the family of solution operators $\{T(t)\}_{t \geq 0}$, defined by $T(t)u_0 = u(t, \cdot, \cdot)$, forms a strongly continuous semigroup of bounded linear operators in the Banach space $L^1(\Omega)$, see [9, Theorem 3.1] or [8, Theorem 2.3].

With the further assumption that μ , α and β are Lipschitz continuous on the interior of their domains, Kang et al. prove in [8, Sections 4 and 5.2] that $\{T(t)\}_{t \geq 0}$ is eventually compact and has asynchronous exponential growth.

*In [8] μ is required to be L^1 on its domain; here we make a different choice to allow for unbounded mortality (see Section 2.1) [28,29]. Accordingly, in order to have a well-posed IG we added a condition on $\mu\phi$ in its domain in (2.6).

The IG of the semigroup $\{T(t)\}_{t \geq 0}$ is the operator $A: D(A) \rightarrow L^1(\Omega)$ defined by

$$A\phi = \lim_{t \rightarrow 0^+} \frac{1}{t}(T(t)\phi - \phi), \quad (2.4)$$

where $D(A) \subset L^1(\Omega)$ consists of the functions for which the limit exists. Kang et al. [8, Remark 2.3] prove that the operator A satisfies

$$\begin{aligned} A\phi(x, y) &= -\partial_x \left[\phi(x, y) + \partial_y \int_{x_0}^x \phi(a, y) da \right] - \mu(x, y)\phi(x, y) \\ &= -\partial_y \left[\phi(x, y) + \partial_x \int_{y_0}^y \phi(x, a) da \right] - \mu(x, y)\phi(x, y), \end{aligned} \quad (2.5)$$

for a.e. $x \in [x_0, \bar{x}]$, a.e. $y \in [y_0, \bar{y}]$, and every $\phi \in D(A)$, and that $D(A)$ satisfies the inclusion

$$\begin{aligned} D(A) \subset & \left\{ \phi \in L^1(\Omega) \mid \mu\phi \in L^1(\Omega), \right. \\ & (x, y) \mapsto \int_{x_0}^x \phi(s, y) ds \text{ is absolutely continuous in } y, \text{ for a.e. } x \in [x_0, \bar{x}], \\ & (x, y) \mapsto \left[\phi(x, y) + \partial_y \int_{x_0}^x \phi(s, y) ds \right] \text{ is absolutely continuous in } x, \text{ for a.e. } y \in [y_0, \bar{y}], \\ & \lim_{x \rightarrow x_0^+} \left[\phi(x, y) + \partial_y \int_{x_0}^x \phi(s, y) ds \right] = K_\beta(\phi)(y) \text{ for a.e. } y \in [y_0, \bar{y}], \\ & (x, y) \mapsto \int_{y_0}^y \phi(x, s) ds \text{ is absolutely continuous in } x, \text{ for a.e. } y \in [y_0, \bar{y}], \\ & (x, y) \mapsto \left[\phi(x, y) + \partial_x \int_{y_0}^y \phi(x, s) ds \right] \text{ is absolutely continuous in } y, \text{ for a.e. } x \in [x_0, \bar{x}], \\ & \lim_{y \rightarrow y_0^+} \left[\phi(x, y) + \partial_x \int_{y_0}^y \phi(x, s) ds \right] = K_\alpha(\phi)(x) \text{ for a.e. } x \in [x_0, \bar{x}], \\ & \partial_x \left[\phi(x, y) + \partial_y \int_{x_0}^x \phi(s, y) ds \right] \in L^1(\Omega), \\ & \left. \partial_y \left[\phi(x, y) + \partial_x \int_{y_0}^y \phi(x, s) ds \right] \in L^1(\Omega) \right\}, \end{aligned} \quad (2.6)$$

while [9, Remark 6.1] claims that equality holds. If $\phi \in D(A)$ is sufficiently smooth, the action (2.5) of the operator A simplifies and can be expressed as

$$A\phi = -(\partial_x \phi + \partial_y \phi + \mu\phi).$$

The spectrum of the IG determines the stability of the null equilibrium.[†] More precisely, the latter is asymptotically stable if and only if the spectral abscissa of A is negative and it is unstable if the spectral abscissa is positive (see [30, Theorem 9.5] and [31, Theorem VI.1.15]).

[†]Note that since A is an operator on a real Banach space, in order to define and compute its spectrum the space and the operator need to be complexified. For details see, e.g., [32, Section III.7].

Observe that in the model defined by (2.1)–(2.3) the structuring variables evolve with the same velocity as time. In Sections 3 and 4 we present the integral reformulation and the discretization restricting to this special case, as in [8]. However, they can be applied to the case of nontrivial velocities as described in Section 6.

2.1. About unbounded mortality

When dealing with structuring variables with finite spans, it is common to require that the mortality becomes unbounded when approaching the maximum values of the structuring variables. As for the case of models with two physiological structures, by defining

$$U(x, y) := \int_0^{\min\{x-x_0, y-y_0\}} \mu(x-s, y-s) ds$$

it is reasonable to require for example that

$$\lim_{x \rightarrow \bar{x}} U(x, y) = \lim_{y \rightarrow \bar{y}} U(x, y) = +\infty.$$

In this case, from a numerical point of view, it can be convenient to argue in terms of $\Pi(x, y) := e^{-U(x, y)}$. It is easy in fact to see that $\Pi(x, y) \rightarrow 0$ for $x \rightarrow \bar{x}$ or $y \rightarrow \bar{y}$. Moreover, by letting $v(t, x, y) := \Pi(x, y)^{-1}u(t, x, y)$, we can observe that if u is a solution of (2.1)–(2.3) with $u(0, x, y) = u_0(x, y)$, then $v(t, x, y)$ solves the PDE

$$\partial_t v(t, x, y) + \partial_x v(t, x, y) + \partial_y v(t, x, y) = 0$$

with boundary conditions

$$\begin{aligned} v(t, x, y_0) &= \iint_{\Omega} \alpha(x, \xi, \sigma) \Pi(\xi, \sigma) v(t, \xi, \sigma) d\xi d\sigma, \\ v(t, x_0, y) &= \iint_{\Omega} \beta(y, \xi, \sigma) \Pi(\xi, \sigma) v(t, \xi, \sigma) d\xi d\sigma, \end{aligned}$$

and $v(0, x, y) = u_0(x, y) \Pi(x, y)^{-1}$.

3. Equivalent formulation in a space of absolutely continuous functions

To conveniently handle the boundary conditions in $D(A)$ from a numerical point of view, inspired by the approach of [16] in the case of one structuring variable, we argue in terms of the integrated state. In particular, we define an isomorphism between $L^1(\Omega)$ and a suitable space of functions via integration. We then use this isomorphism and the semigroup $\{T(t)\}_{t \geq 0}$ to construct an appropriate semigroup acting on a space of functions with higher regularity. With this goal in mind, we first recall the definition and some properties of absolute continuity in the sense of Carathéodory. We refer the reader to [33] for further details.

A function v defined on Ω is *absolutely continuous in the sense of Carathéodory* if and only if there exist $e_v \in \mathbb{R}$, $f_v \in L^1([x_0, \bar{x}])$, $g_v \in L^1([y_0, \bar{y}])$ and $h_v \in L^1(\Omega)$ such that

$$v(x, y) = e_v + \int_{x_0}^x f_v(a) da + \int_{y_0}^y g_v(b) db + \int_{x_0}^x \int_{y_0}^y h_v(a, b) db da.$$

Observe that the iterated integral in the last term is equal to the double integral on $[x_0, x] \times [y_0, y]$ and to the iterated integral on the variables a and b in the opposite order, thanks to Fubini's theorem. The space $AC(\Omega)$ of absolutely continuous functions on Ω in the sense of Carathéodory is a Banach space when equipped with the norm $\|\cdot\|_{AC(\Omega)}$ defined as

$$\|v\|_{AC(\Omega)} := |e_v| + \|f_v\|_{L^1([x_0, \bar{x}])} + \|g_v\|_{L^1([y_0, \bar{y}])} + \|h_v\|_{L^1(\Omega)}.$$

We consider a particular subspace of $AC(\Omega)$, namely

$$AC_0(\Omega) := \left\{ v: \Omega \rightarrow \mathbb{R} \mid v(x, y) = \int_{x_0}^x \int_{y_0}^y h_v(a, b) db da \text{ for some } h_v \in L^1(\Omega) \right\}.$$

Observe that $AC_0(\Omega)$ is a Banach space, being a closed subspace, and that $v(x_0, y) = v(x, y_0) = 0$ for $v \in AC_0(\Omega)$. The operator $V: L^1(\Omega) \rightarrow AC_0(\Omega)$ defined by

$$V\phi(x, y) = \int_{x_0}^x \int_{y_0}^y \phi(a, b) db da$$

defines an isomorphism between $L^1(\Omega)$ and $AC_0(\Omega)$, with $V^{-1}\psi = \partial_x \partial_y \psi$ for all $\psi \in AC_0(\Omega)$. Observe that both V and V^{-1} are bounded ($\|V\| = \|V^{-1}\| = 1$).

Note that, given a solution u of (2.1)–(2.3), $\int_{x_0}^x \int_{y_0}^y u(t, a, b) db da$ represents the number of individuals whose structuring variables belong to $[x_0, x] \times [y_0, y]$ at time t .

Returning now to (2.1)–(2.3), we define the family of operators $\{S(t)\}_{t \geq 0}$ on $AC_0(\Omega)$ as $S(t) := VT(t)V^{-1}$. Since V and V^{-1} are linear and bounded, the operators $S(t)$ are in turn linear and bounded and form a family with the same properties as $\{T(t)\}_{t \geq 0}$, namely they form a strongly continuous semi-group on $AC_0(\Omega)$. Its IG is $B: D(B) \rightarrow AC_0(\Omega)$, with $B := VAV^{-1}$ and $D(B) = VD(A)$.

With the aim of using B to study the stability properties of (2.1)–(2.3), it is important to understand the relation between the spectra of A and B . First of all, from $B = VAV^{-1}$ we can write $B - \lambda I = V(A - \lambda I)V^{-1}$ for any $\lambda \in \mathbb{C}$. This implies that the resolvent sets of A and B , and consequently their spectra, coincide. Moreover, $\phi \in L^1(\Omega)$ is an eigenvector of A if and only if $V\phi \in AC_0(\Omega)$ is an eigenvector of B corresponding to the same eigenvalue. Thus, given the invertibility of V , A and B also share the same eigenvalues (with the same multiplicity). Eventually, from the statements (i) and (iv) in [8, Proposition 5.6], as well as the proof of (v), we can conclude that the spectrum of A only consists of eigenvalues, which implies that the same holds for B . From [8, Proposition 3.1], noting that in that proof $\chi = A\phi + \mu\phi$, for $\psi \in D(B)$ we can write

$$\begin{aligned} B\psi(x, y) &= -\partial_x \psi(x, y) - \partial_y \psi(x, y) \\ &+ \int_{x_0}^x K_\alpha(\partial_y \partial_x \psi)(a) da + \int_{y_0}^y K_\beta(\partial_y \partial_x \psi)(b) db \\ &- \int_{x_0}^x \int_{y_0}^y \mu(a, b) \partial_y \partial_x \psi(a, b) db da. \end{aligned} \tag{3.1}$$

4. Pseudospectral discretization of the IG

In this Section, we use pseudospectral methods with a tensorial approach to obtain a finite-dimensional approximation of the operator B , whose spectrum can be used to determine the stability properties of the system.

For n and m positive integers, let $\Pi_{n,m}^0$ be the space of bivariate polynomials on Ω of degree at most n in the first variable and at most m in the second variable, taking value 0 at $x = x_0$ and $y = y_0$. These conditions are motivated by the fact that we use polynomials in $\Pi_{n,m}^0$ as approximations of functions in $AC_0(\Omega)$. Let $\Theta_X = \{x_1, \dots, x_n\}$ be a mesh of n points in $(x_0, \bar{x}]$, with $x_0 < x_1 < \dots < x_n = \bar{x}$, and let $\Theta_Y = \{y_1, \dots, y_m\}$ be a mesh of m points in $(y_0, \bar{y}]$, with $y_0 < y_1 < \dots < y_m = \bar{y}$. We approximate a function $\psi \in AC_0(\Omega)$ by a vector $\Psi \in \mathbb{R}^{nm}$ according to

$$\psi(x_i, y_j) = \Psi_{i,j}, \quad i = 1, \dots, n, \quad j = 1, \dots, m,$$

where the components of Ψ are ordered according to the lexicographic order of the double indices (i, j) .

Given $\Psi \in \mathbb{R}^{nm}$, let $\psi_{n,m} \in \Pi_{n,m}^0$ be the polynomial interpolating Ψ on $\Theta_X \times \Theta_Y$:

$$\psi_{n,m}(x_i, y_j) = \Psi_{i,j}, \quad i = 1, \dots, n, \quad j = 1, \dots, m.$$

The finite-dimensional approximation of the operator B is then $B_{n,m}: \mathbb{R}^{nm} \rightarrow \mathbb{R}^{nm}$ defined as

$$[B_{n,m}\Psi]_{i,j} := (B\psi_{n,m})(x_i, y_j), \quad i = 1, \dots, n, \quad j = 1, \dots, m. \quad (4.1)$$

We can write more explicitly the entries of the matrix $B_{n,m}$ by using the bivariate Lagrange representation of $\psi_{n,m}$, together with the explicit action of the operator B defined in (3.1). Let $\{\ell_{X,i}\}_{i=0,\dots,n}$ and $\{\ell_{Y,j}\}_{j=0,\dots,m}$ be the Lagrange bases of polynomials relevant to $\{x_0\} \cup \Theta_X$ and $\{y_0\} \cup \Theta_Y$, i.e.,

$$\ell_{X,i}(x) = \prod_{\substack{k=0 \\ k \neq i}}^n \frac{x - x_k}{x_i - x_k}, \quad \ell_{Y,j}(y) = \prod_{\substack{k=0 \\ k \neq j}}^m \frac{y - y_k}{y_j - y_k}.$$

The polynomial $\psi_{n,m}$ can be written as

$$\psi_{n,m}(x, y) = \sum_{i=1}^n \sum_{j=1}^m \ell_{X,i}(x) \ell_{Y,j}(y) \Psi_{i,j}, \quad (x, y) \in \Omega.$$

Note that indeed $\psi_{n,m}(x, y) = 0$ for $x = x_0$ or $y = y_0$. Using (3.1) and (4.1), we get

$$\begin{aligned} [B_{n,m}\Psi]_{k,l} &= - \sum_{i=1}^n \ell'_{X,i}(x_k) \Psi_{i,l} - \sum_{j=1}^m \ell'_{Y,j}(y_l) \Psi_{k,j} \\ &+ \int_{y_0}^{y_l} K_\beta \left(\sum_{i=1}^n \sum_{j=1}^m \ell'_{X,i} \ell'_{Y,j} \Psi_{i,j} \right) (b) db \\ &+ \int_{x_0}^{x_k} K_\alpha \left(\sum_{i=1}^n \sum_{j=1}^m \ell'_{X,i} \ell'_{Y,j} \Psi_{i,j} \right) (a) da \\ &- \int_{x_0}^{x_k} \int_{y_0}^{y_l} \mu(a, b) \sum_{i=1}^n \sum_{j=1}^m \ell'_{X,i}(a) \ell'_{Y,j}(b) \Psi_{i,j} db da. \end{aligned}$$

Using the linearity of K_α and K_β , it is easy to characterize the entries of the matrix $B_{n,m}$. Let $D_X \in \mathbb{R}^{n \times n}$ and $D_Y \in \mathbb{R}^{m \times m}$ be defined as

$$[D_X]_{i,j} = \ell'_{X,j}(x_i), \quad i, j = 1, \dots, n$$

$$[D_Y]_{i,j} = \ell'_{Y,j}(y_i), \quad i, j = 1, \dots, m.$$

In other words, D_X and D_Y are the part of the differentiation matrices associated with $\{x_0\} \cup \Theta_X$ and $\{y_0\} \cup \Theta_Y$, respectively, deleting the first row and the first column. The bivariate differentiation matrices in x and y are

$$\mathbf{D}_X = D_X \otimes I_m, \quad \mathbf{D}_Y = I_n \otimes D_Y,$$

where \otimes denotes the Kronecker product. We can then write

$$B_{n,m} = -\mathbf{D}_X - \mathbf{D}_Y + \mathbf{A} + \mathbf{B} - \mathbf{M},$$

where $\mathbf{A}, \mathbf{B}, \mathbf{M} \in \mathbb{R}^{nm \times nm}$ are defined by

$$\mathbf{A}_{(k,l),(i,j)} = \int_{x_0}^{x_k} K_\alpha(\ell'_{X,i} \ell'_{Y,j})(a) da, \quad (4.2)$$

$$\mathbf{B}_{(k,l),(i,j)} = \int_{y_0}^{y_l} K_\beta(\ell'_{X,i} \ell'_{Y,j})(b) db, \quad (4.3)$$

$$\mathbf{M}_{(k,l),(i,j)} = \int_{x_0}^{x_k} \int_{y_0}^{y_l} \mu(a, b) \ell'_{X,i}(a) \ell'_{Y,j}(b) db da, \quad (4.4)$$

for $k, i = 1, \dots, n$ and $l, j = 1, \dots, m$. Note that, if μ is constant, the matrix \mathbf{M} is diagonal with diagonal entries equal to μ .

We finally note that, although the matrix $B_{n,m}$ is defined for any set of nodes, the choice of the latter is critical to ensure the convergence of the interpolating polynomials and, in turn, of the elements of the spectrum. In the following numerical experiments, we choose the Chebyshev extremal points in each interval $[x_0, \bar{x}]$ and $[y_0, \bar{y}]$.

In the univariate case, these nodes guarantee that the convergence rate of the interpolating polynomial of degree n is $O(n^{-k})$ if the interpolated function is C^k [17, Theorem 7.2], which implies that the order of convergence is infinite if the function is smooth. Moreover, the convergence rate is $O(c^n)$ for some $0 < c < 1$ if the function is analytic [17, Theorem 8.2]. The two latter properties are often known as *spectral accuracy*, see [34, chapter 4] and [35, chapter 2]. Furthermore, observe that the relevant differentiation matrices can be computed explicitly [34].

The classic result on the interpolation error being bounded by means of the best uniform approximation error and the Lebesgue constant holds also in the bivariate case. A multidimensional version of Jackson's theorem on the best uniform approximation error holds as well [36, Theorem 4.8]. Moreover, it is easy to verify that the Lebesgue constant for the tensor-product Chebyshev extremal nodes in Ω is the product of the univariate Lebesgue constants in $[x_0, \bar{x}]$ and $[y_0, \bar{y}]$, hence it is $O(\log n \log m)$. The tensor-product Chebyshev interpolation is thus near-optimal also in the bivariate case.

Although a proof of convergence for the method is out of the scope of this paper, we show that the order of convergence observed numerically for the approximated eigenvalues and eigenvectors is consistent with the well-established order of convergence of polynomial interpolation.

For implementation purposes, we observe that in general the integrals defining \mathbf{A} , \mathbf{B} and \mathbf{M} in (4.2)–(4.4) cannot be computed exactly. To approximate the integrals on Ω we use the Clenshaw–Curtis cubature formula [37], which is based on Chebyshev extremal points and is spectrally accurate [34, 38].

To compute the entries of \mathbf{A} and \mathbf{B} , given a function f defined on $[x_0, \bar{x}]$ and $F \in \mathbb{R}^n$ such that $F_i = f(x_i)$, we consider the approximation

$$\int_{x_0}^{x_k} f(a) da \approx [D_{\bar{x}}^{-1}F]_k, \quad k = 1, \dots, n,$$

and similarly for functions defined on $[y_0, \bar{y}]$ (see, e.g., [45]). This approximation can be extended to the double integrals involved in the entries of the matrix \mathbf{M} for nonconstant μ . More precisely, given a function $\psi \in AC_0(\Omega)$ and a vector $\Psi \in \mathbb{R}^{nm}$ such that $\Psi_{k,l} = \psi(x_k, y_l)$, each integral $\int_{x_0}^{x_k} \int_{y_0}^{y_l} \psi(a, b) da db$ can be approximated by the corresponding (k, l) -th entry of the vector $\mathbf{D}_X^{-1} \mathbf{D}_Y^{-1} \Psi$.

5. Numerical experiments

In this Section, we present several numerical experiments to investigate how the spectrum of the finite-dimensional operator $B_{n,m}$ approximates the spectrum of B , and in turn of A , of each problem at hand. For this purpose, we select several parameter sets for which eigenvalues and eigenfunctions of A can be expressed explicitly, and we study the convergence of the approximated eigenvalues of $B_{n,m}$ to the analytic ones. As for the eigenfunctions, we stress that, since $B_{n,m}$ represents an approximation of the operator B , an eigenvector Ψ of $B_{n,m}$ provides an approximation $\psi_{n,m}$ of $V\phi$, where ϕ is an eigenfunction of A ; an approximation of ϕ is thus given by $\partial_x \partial_y \psi_{n,m}$.

For each example we study the behavior for increasing $n = m$ of the absolute error ϵ_λ on the known eigenvalue λ and of the absolute error ϵ_ϕ in L^1 norm on the known eigenfunction ϕ , computed via Clenshaw–Curtis cubature.

In all examples we choose

$$\alpha(x, \xi, \sigma) = \alpha_1(x)\gamma(\xi, \sigma), \quad \beta(y, \xi, \sigma) = \beta_1(y)\gamma(\xi, \sigma)$$

in the boundary conditions (2.2)–(2.3), in order to simplify finding an explicit eigenfunction.

We remark that the parameters are chosen in order to have an analytically known eigenfunction with certain smoothness properties, without regard to any specific biological interpretation.

To compute the spectrum of $B_{n,m}$ we use standard methods (namely MATLAB's `eig` function). Note that the approximated spectrum may contain spurious eigenvalues (e.g., when B has fewer eigenvalues than the dimension of $B_{n,m}$); however, in our examples we only examine specific eigenvalues, so that the spurious ones do not affect our analysis.

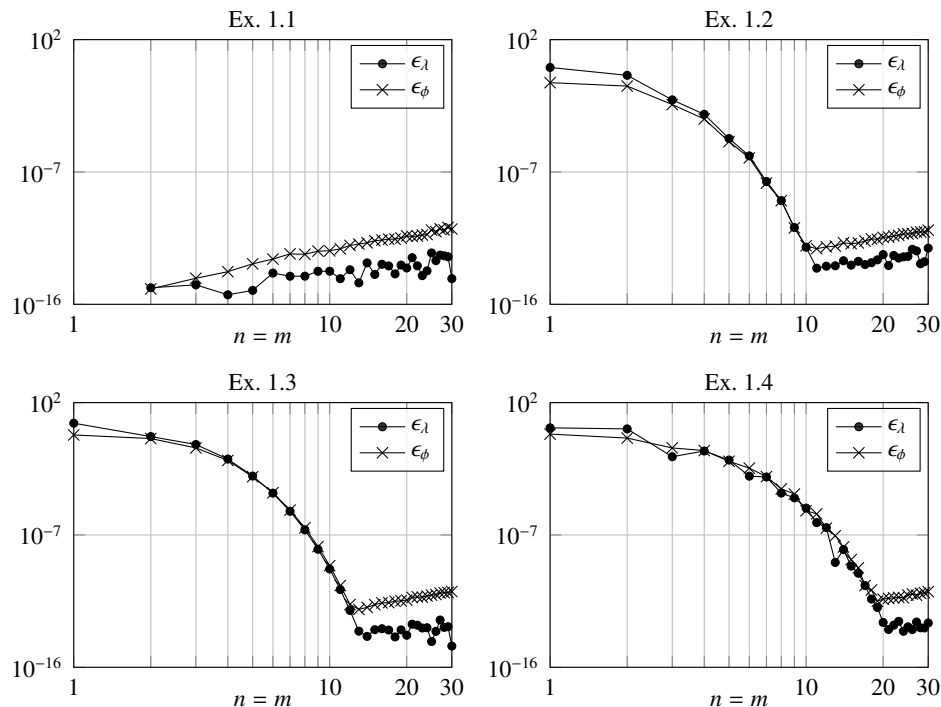
5.1. Analytic eigenfunctions

We consider a first group of examples presenting an analytic eigenfunction. The choices of the parameters and the resulting eigenvalue and eigenfunction are listed in Table 1. Starting from Example 1.1, where all parameters are constant, we gradually introduce nonconstant coefficients: α_1 and β_1 in Example 1.2, γ in Example 1.3 and μ in Example 1.4.

Considering Example 1.1, Figure 1 shows that the errors reach the machine precision already for $n = m = 2$. With $n = m = 1$ the errors are exactly equal to 0, which may be explained by the fact that constant functions are interpolated exactly already by polynomials of degree 0. As $n = m$ increases, the errors increase, possibly due to numerical instability.

Table 1. Parameters and resulting eigenvalue and eigenfunction in the analytic cases.

	Ex. 1.1	Ex. 1.2	Ex. 1.3	Ex. 1.4
Ω	$[0, 1]^2$	$\left[\frac{\pi}{6}, \frac{\pi}{2}\right] \times \left[\frac{\pi}{6}, \frac{\pi}{4}\right]$	$[0, 2] \times [-1, 1]$	$[0, 2] \times [0, 1]$
$\alpha_1(x)$	1	$\cos(x - \frac{\pi}{6})$	e^{x+1}	e^{-x^2}
$\beta_1(y)$	1	$\cos(\frac{\pi}{6} - y)$	e^{-y}	e^y
$\gamma(\xi, \sigma)$	1	$\left(\frac{\sqrt{2}-\sqrt{6}+2}{4}\right)^{-1}$	$\frac{1}{4}e^{-\xi+\sigma}$	$\left(\iint_{\Omega} e^{-a^2+b} db da\right)^{-1}$
$\mu(x, y)$	1	1	1	$2x + 1$
λ	-1	-1	-1	-2
$\phi(x, y)$	1	$\cos(x - y)$	e^{x-y}	e^{-x^2+y}

Figure 1. Errors ϵ_λ and ϵ_ϕ for Examples 1.1, 1.2, 1.3 and 1.4 defined in Table 1. Observe that for Example 1.1 with $n = m = 1$ the errors are exactly 0, hence they are not represented in the logarithmic scale.

Considering now Examples 1.2, 1.3 and 1.4, Figure 1 shows that both ϵ_λ and ϵ_ϕ decay with infinite order. Observe that in Example 1.4 more nodes are needed to reach the error barrier than in Examples 1.2 and 1.3, probably due to the approximation of the integrals involving the nonconstant μ .

5.2. Nonsmooth eigenfunctions

Table 2. Parameters and resulting eigenvalue and eigenfunction in the nonsmooth case. $\mathbf{1}_A$ is the indicator function of $A \subset \mathbb{R}$. The regularity of the eigenfunction is shown in parentheses in the titles.

	Ex. 2.1 (C^2)	Ex. 2.2 (C^1)	Ex. 2.3 (C^0)	Ex. 2.4 (discontinuous)
Ω	$[0, 1] \times [0, 2]$	$[0, 1] \times [0, 2]$	$[0, 1] \times [0, 2]$	$[0, 1] \times [0, 2]$
$\alpha_1(x)$	$x^2 x $	$-x x $	$ x $	$\mathbf{1}_{[0,+\infty[}(x)$
$\beta_1(y)$	$y^2 y $	$y y $	$ y $	$\mathbf{1}_{]-\infty,0]}(y)$
$\gamma(\xi, \sigma)$	$\frac{5}{8}$	$\frac{6}{7}$	$\frac{3}{4}$	2
$\mu(x, y)$	1	1	1	1
λ	-1	-1	-1	-1
$\phi(x, y)$	$(x - y)^2 x - y $	$(x - y) x - y $	$ x - y $	$\mathbf{1}_{[0,+\infty[}(x - y)$

For the second group of examples, we consider eigenfunctions which are not smooth. The choices of the parameters and the resulting eigenvalue and eigenfunction are listed in Table 2. Observe that the eigenfunctions have the same regularity as the coefficients α_1 and β_1 , namely C^2 for Example 2.1, C^1 for Example 2.2 and C^0 for Example 2.3. We consider also Example 2.4 with discontinuous coefficients and eigenfunction.

Figure 2 suggests that the errors decay with finite order and these orders increase with the regularity of the eigenfunction. In particular, we can observe that for both errors a loss of one order of differentiability, or the loss of continuity, of the eigenfunction seems to correspond to a loss of about one order of convergence (cfr. the dashed reference lines in Figure 2). The convergence of ϵ_λ seems to be almost two orders faster than that of ϵ_ϕ . To possibly explain this difference, recall that we are actually collocating the eigenvalue problem for B , which means that the eigenvalues are the same as A , but the eigenfunctions correspond to integrals of the eigenfunctions of A , so the comparison between the eigenfunctions involves differentiating the computed ones.

6. Structuring variables with nontrivial velocity

We have illustrated the method for systems in which both physiological variables evolve at the same velocity as time. This should not be seen as too restrictive, as systems with more general velocity terms [1-5] can in some cases be reduced to (2.1)–(2.3) after a suitable scaling of variables, so that similar theoretical results on the stability of the null solution hold [9]. In practice, however, the computation

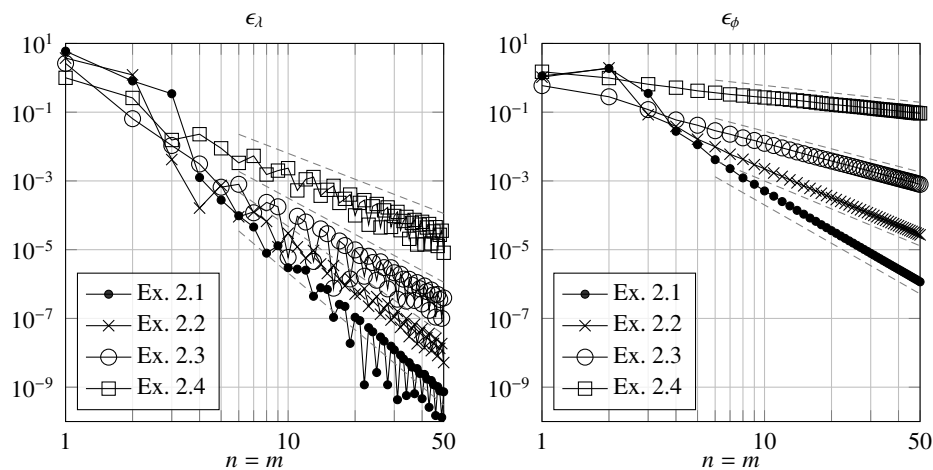


Figure 2. Errors ϵ_l (left) and ϵ_ϕ (right) for Examples 2.1, 2.2, 2.3 and 2.4 defined in Table 2. The slopes of the dashed gray lines are -2.5 , -3.5 , -4.5 , -5.5 (left) and -0.7 , -1.7 , -2.7 , -3.7 (right), included to ease the interpretation of the plots.

of the change of variables, which in general is defined by the solution of an ODE system, may be expensive, although necessary when the individual parameters (e.g., birth and mortality rates) depend on the original (unscaled) variables. In this case, directly approximating the original problem with nontrivial velocities may be convenient from a computational point of view, as observed in [16].

In fact, the transformation via integration can be easily carried out for problems of the form

$$\begin{aligned} \partial_t u(t, x, y) + \partial_x(g_X(x)u(t, x, y)) + \partial_y(g_Y(y)u(t, x, y)) &= -\mu(x, y)u(t, x, y), \\ g_Y(y_0)u(t, x, y_0) &= K_\alpha(u(t, \cdot, \cdot))(x), \\ g_X(x_0)u(t, x_0, y) &= K_\beta(u(t, \cdot, \cdot))(y), \end{aligned}$$

where the positive functions $g_X(x)$ and $g_Y(y)$ describe the rates of change of x and y in time. In this case, it is straightforward to verify that, given the IG A , the operator $B = VAV^{-1}$ admits the representation

$$\begin{aligned} B\psi(x, y) &= -g_X(x)\partial_x\psi(x, y) - g_Y(y)\partial_y\psi(x, y) \\ &+ \int_{x_0}^x K_\alpha(\partial_y\partial_x\psi)(a) da + \int_{y_0}^y K_\beta(\partial_y\partial_x\psi)(b) db \\ &- \int_{x_0}^x \int_{y_0}^y \mu(a, b)\partial_y\partial_x\psi(a, b) db da, \end{aligned}$$

which is approximated by a matrix of the form

$$B_{n,m} = -\mathbf{G}_X \mathbf{D}_X - \mathbf{G}_Y \mathbf{D}_Y + \mathbf{A} + \mathbf{B} - \mathbf{M},$$

where \mathbf{A} , \mathbf{B} and \mathbf{M} are the matrices defined in Section 4 and $\mathbf{G}_X = G_X \otimes I_m$, $\mathbf{G}_Y = I_n \otimes G_Y$, with G_X and G_Y diagonal matrices defined by $[G_X]_{i,i} = g_X(x_i)$, $i = 1, \dots, n$, and $[G_Y]_{j,j} = g_Y(y_j)$, $j = 1, \dots, m$.

As an example let us consider

$$\Omega := \left[\frac{1}{2}, \frac{3}{2} \right] \times \left[\frac{1}{2}, 2 \right], \quad g_X(x) := x, \quad g_Y(y) := \frac{y^2}{2},$$

$$\mu(x, y) := y^3 - 2x^2 - y + 4,$$

$$\alpha(x, \xi, \sigma) := \frac{e^{x^2 - \frac{1}{4}}}{8c}, \quad \beta(y, \xi, \sigma) := \frac{e^{-y^2 + \frac{1}{4}}}{2c}, \quad c = \frac{1}{4}\pi \iint_{\Omega} e^{a^2 - b^2} da db,$$

for which $\lambda = -5$ is an eigenvalue of the corresponding IG with eigenfunction $\phi(x, y) = e^{x^2 - y^2}$. We can observe in Figure 3 that the errors decay with infinite order even in this case.

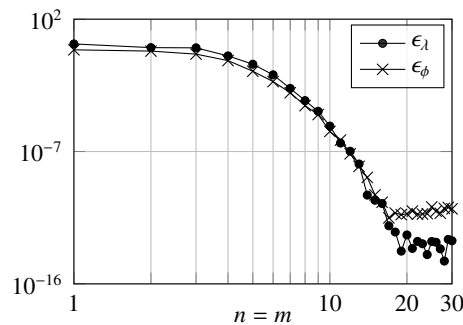


Figure 3. Errors ϵ_λ and ϵ_ϕ for the example of Section 6.

7. Applications

7.1. An epidemiological model structured by age and time since infection

We now consider an epidemic reinfection model proposed in [6] with individuals structured by demographic (or chronological) age $a \in [0, a^\dagger]$ and time since infection $\tau \in [0, \tau^\dagger]$. All individuals are assumed to experience a natural mortality $\mu(a)$, and we define the corresponding survival probability

$$\ell(a) := \exp\left(-\int_0^a \mu(\sigma) d\sigma\right)$$

and the average life expectancy of individuals

$$e_0 := \int_0^{a^\dagger} \ell(a) da.$$

Susceptible individuals can become infected upon contact with an infectious individual at a rate given by $\beta(\tau)$. Infected individuals recover at a rate $\gamma(\tau)$. After linearization around the disease-free steady state, the linear equation for the infected individuals reads

$$\partial_t \zeta(t, \tau, a) + \partial_\tau \zeta(t, \tau, a) + \partial_a \zeta(t, \tau, a) = -(\mu(a) + \gamma(\tau))\zeta(t, \tau, a), \quad \tau \in [0, \tau^\dagger], \quad a \in [0, a^\dagger],$$

$$\zeta(t, 0, a) = w^*(a) \int_0^{\tau^\dagger} \int_0^a \beta(\tau)\zeta(t, \tau, \sigma) d\sigma d\tau,$$

$$\zeta(t, \tau, 0) = 0,$$

where $\zeta(t, \tau, a)$ is the density of the infected individuals in the linearization around the disease-free steady state and $w^*(a) = \ell(a)/e_0$ is the age profile of the host population in the demographic steady state.

Following [6, Section 4.2], the reproduction number is given by

$$R_0 = \int_0^{a^\dagger} \Psi(a)w^*(a) da,$$

with

$$\Psi(a) := \int_0^{\min\{a^\dagger - a, \tau^\dagger\}} \beta(\tau)\Gamma(\tau)\frac{\ell(a + \tau)}{\ell(a)} d\tau, \quad \Gamma(\tau) := \exp\left(-\int_0^\tau \gamma(\sigma) d\sigma\right).$$

Observe that $\Gamma(\tau)$ is the probability of an individual not being removed before time since infection τ . Hence we expect the disease-free equilibrium to undergo a bifurcation at $R_0 = 1$ and specifically we expect a real eigenvalue crossing the imaginary axis from left to right.

Table 3. Parameters for the analysis of the epidemic model of Section 7.1. In the computations we approximate 1 year as 52 weeks.

Symbol	Value	Description
a^\dagger	100 years	Maximal age
τ^\dagger	2 weeks	Maximal infectious period
$\beta(\tau)$	varying $\beta_0 > 0$	Infectivity profile
$\mu(a)$	$\frac{1}{a^\dagger - a}$	Natural mortality
$\gamma(\tau)$	$\frac{1}{\tau^\dagger - \tau}$	Removal rate of infected individuals

For the numerical simulations we use parameters as in Table 3, which are simplified parameters but broadly consistent with a short infection like COVID-19. For this choice of parameters, $R_0 = \beta_0/k$ with

$$k := \frac{81120000}{40549601} \approx 2.0005. \quad (7.1)$$

Since discretizing a large interval causes slower convergence of interpolation methods, for the purpose of the numerical experiments we rescale the variables to the interval $[0, 1]$ considering new variables $x := \tau/\tau^\dagger$ and $y := a/a^\dagger$ and $u(t, x, y) := \zeta(t, \tau, a)$. The resulting model reads

$$\begin{aligned} \partial_t u(t, x, y) + \frac{1}{\tau^\dagger} \partial_x u(t, x, y) + \frac{1}{a^\dagger} \partial_y u(t, x, y) &= -(\mu(a^\dagger y) + \gamma(\tau^\dagger x))u(t, x, y), \quad x, y \in [0, 1], \\ u(t, 0, y) &= w^*(a^\dagger y) \int_0^1 \int_0^y \beta(\tau^\dagger x)u(t, x, \sigma)\tau^\dagger a^\dagger dx d\sigma, \\ u(t, x, 0) &= 0. \end{aligned}$$

We further apply to this model the reformulation described in 2.1 to avoid issues with the unboundedness of μ and γ .

Figure 4 shows the rightmost part of the spectrum of the IG for values of R_0 around the bifurcation at $R_0 = 1$: as anticipated, the rightmost eigenvalue is real and crosses the imaginary axis. The figure shows the eigenvalues of the IG discretized with two different values of $n = m$: the comparison suggests that some of the eigenvalues are spurious, more precisely the ones seemingly not lying on the emerging exponential-like curves (excluding, of course, the spectral abscissa).

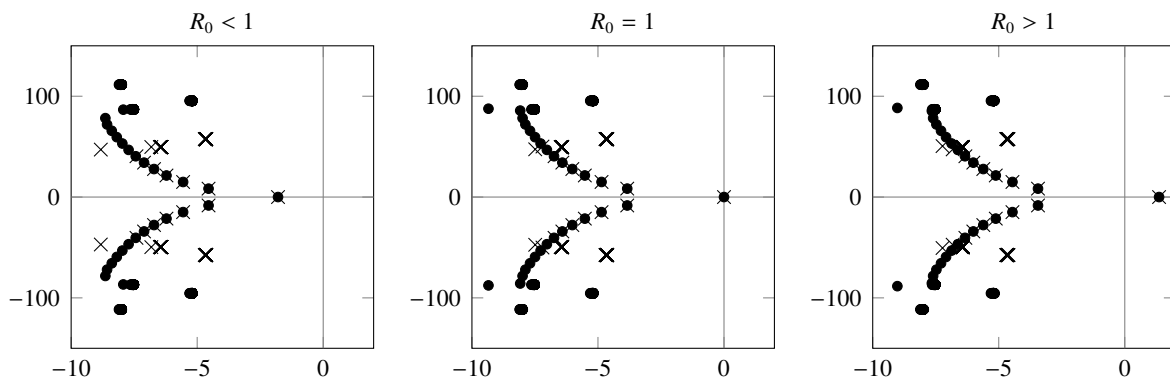


Figure 4. Eigenvalues of the IG with real part greater than -10 with $\beta_0 = k - 1$, $\beta_0 = k$ and $\beta_0 = k + 1$, with k as in (7.1), corresponding respectively to $R_0 < 1$, $R_0 = 1$ and $R_0 > 1$, computed with $n = m = 30$ (\times) and with $n = m = 50$ (\bullet).

7.2. A population model structured by age and size

To further illustrate the efficacy of the method on realistic models with nontrivial velocity, we consider a model inspired from ecology, with individuals structured by their demographic age a and their size z , which grows in time with velocity $g(z)$ [7]. We will take parameters inspired by the *Daphnia* population growth model [12, 39], but assuming that the algae resource is fixed at a certain value. We consider a slight modification of parameters so that both the survival probability at the maximal age and the growth rate at the maximal size are zero. We consider $a \in [0, a^\dagger]$ and $z \in [z_b, z_m]$ with parameters as in Table 4.

We assume that individuals start reproducing after reaching the reproductive size z_A . Their offspring's size is distributed according to a density function $w(z)$ with support in $[z_b, z_A]$. The model for the population density $n(t, a, z)$ reads

$$\partial_t n(t, a, z) + \partial_a n(t, a, z) + \partial_z (g(z)n(t, a, z)) = -\mu(a)n(t, a, z), \quad a \in [0, a^\dagger], \quad z \in [z_b, z_m],$$

$$n(t, 0, z) = w(z) \int_0^{a^\dagger} \int_{z_b}^{z_m} \beta(\sigma)n(t, a, \sigma) \, d\sigma \, da,$$

$$n(t, a, 0) = 0.$$

For studying the model we can define $\Pi(a) = \exp(-\int_0^a (\mu(\xi) - \mu_0) \, d\xi)$ and $q(t, a, z) := \Pi(a)^{-1}n(t, a, z)$. Then it is easy to see that q satisfies

$$\partial_t q(t, a, z) + \partial_a q(t, a, z) + \partial_z (g(z)q(t, a, z)) = -\mu_0 q(t, a, z),$$

$$q(t, 0, z) = w(z) \int_0^{a^\dagger} \int_{z_b}^{z_m} \beta(\sigma)\Pi(a)q(t, a, \sigma) \, d\sigma \, da,$$

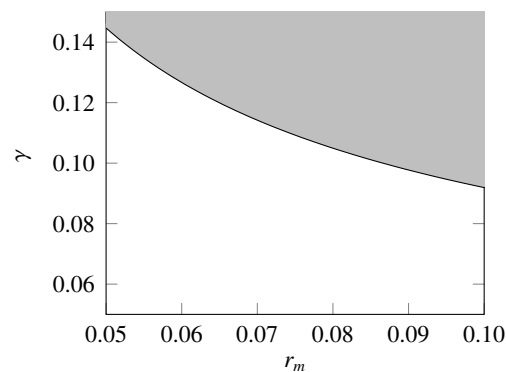
$$q(t, a, 0) = 0.$$

Moreover, we rescale the age variable to the interval $[0, 1]$ as in Section 7.1.

Figure 5 shows the stability chart for the null equilibrium in the parameters r_m and γ , while Figure 6 shows the value of the spectral abscissa varying those two parameters separately.

Table 4. Parameters for the analysis of the population model of Section 7.2.

Symbol	Value	Description
a^\dagger	70	Maximal age
z_b	0.8	Minimal size
z_A	2.5	Maturation size
z_m	6.0	Maximal size
$\mu(a)$	$\mu_0 + \frac{1}{a^\dagger - a}$	Natural mortality
$g(z)$	$\gamma(z_m - z)$	Growth rate in size
$\beta(z)$	$\mathbf{1}_{[z_A, z_m]} \cdot r_m(z - z_A)^2$	Fertility rate
$w(z)$	$\mathbf{1}_{[z_b, z_A]} \cdot (z_A - z)/(z_A - z_b)$	Size distribution of offspring
μ_0	0.7	Mortality constant
γ	varying from 0.05 to 0.15	Growth rate constant
r_m	varying from 0.05 to 0.1	Fertility constant

**Figure 5.** Stability chart for the null equilibrium of the population model of Section 7.2 in the parameters r_m and γ , computed with $n = m = 30$. The black line is the boundary between the stable (white) and unstable (gray) regions.

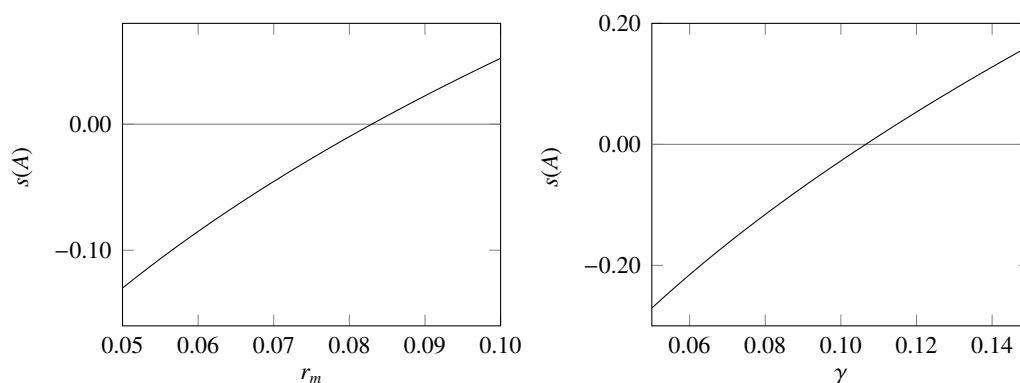


Figure 6. Spectral abscissa of the IG of the population model of Section 7.2 as a function of the parameters r_m with $\gamma = 0.1$ (left) and γ with $r_m = 0.075$ (right), computed with $n = m = 30$.

8. Concluding remarks

In this paper we proposed a numerical technique to analyze the stability of the null solution of linear population models with two structuring variables, of the type considered in [8, 9].

Extensive numerical tests illustrate the convergence of the eigenvalues of the finite-dimensional approximation to the true eigenvalues of the IG. The numerical tests support the conjecture that the order of convergence of the approximation depends on the regularity of the eigenfunction. A rigorous theoretical proof of the convergence of the approximation is left to future work.

Stability analysis requires not only that the eigenvalues of the IG are approximated accurately, but also that no spurious eigenvalues are to the right of the true spectral abscissa. In fact, in our examples we observe that the approximation of the known eigenvalue is the numerical spectral abscissa, suggesting that the method can be effectively used to study the stability.

Structured population models can also be formulated as renewal equations for the population birth rate (or “recruitment function”) [40–42]. The renewal equation formulation is particularly convenient from the theoretical point of view as one can exploit the principle of linearized stability for nonlinear equations, which can not be proved in general for the PDE formulation [40]. Results on the asymptotic behavior of solutions have also been recently proved, under special assumptions, for renewal equations defined on a space of measures, which makes it possible to consider a wider set of solutions compared to PDEs [43, 44].

It would be interesting to apply pseudospectral methods in the framework of renewal equations (admitting a state space of multivalued functions or even measures), by extending the techniques developed for scalar renewal equations [11, 22, 25]. However, when the structuring variables evolve with nontrivial velocity, the renewal equation formulation requires to explicitly invert the age-structure relation defined implicitly by an ODE system, which suffers from the computational challenges highlighted in Section 6. Hence, as explained therein, directly tackling the PDE formulation may be computationally convenient, as it bypasses the solution of the ODE system.

In this paper we restricted to structuring variables in bounded intervals, as this allows to exploit the

highly desirable convergence properties of polynomial interpolation on Chebyshev nodes. However, unbounded domains are common in the modeling literature (e.g., [1, 2, 27, 29]), for instance when it is not easy to determine a suitable upper bound for a physiological variable *a priori*, or when the processes are naturally described by probability distributions with unbounded support (e.g., exponential or Gamma distributions).

In order to numerically treat these problems, truncating the domain can be feasible sometimes, but the accuracy of the approximation would depend on both the size of the truncated domain and the number of nodes in the domain. The latter usually becomes very large because the choice of Chebyshev nodes does not exploit the specific characteristics of the solutions, which usually belong to exponentially weighted spaces [40]. For this reason, using exponentially weighted interpolation and Laguerre-type nodes has proved successful and more efficient than domain truncation in the case of delay equations [26, 46]. It would be interesting to apply similar techniques [35] to structured models in the PDE formulation with one or even two structuring variables, although the latter brings in additional complications due to the necessity to rely on multivariate interpolation.

A. Models with one structuring variable

As recalled in the introduction, [14] already provides a pseudospectral method, based on a different approach, to approximate the IG of models with one structuring variable. In this appendix, for completeness, we adapt our approach to this case, providing also an example.

We consider the scalar first-order linear hyperbolic PDE

$$\partial_t u(t, x) + \partial_x u(t, x) = -\mu(x)u(t, x), \quad (\text{A.1})$$

with boundary condition

$$u(t, x_0) = \int_{x_0}^{\bar{x}} \beta(\sigma)u(t, \sigma) d\sigma =: K_\beta(u(t, \cdot)). \quad (\text{A.2})$$

As references on single structure models, see [28, 29, 47]; in particular, see [29, Section 1.2] for what concerns this appendix.

If $\mu, \beta: [x_0, \bar{x}] \rightarrow \mathbb{R}$ are nonnegative functions with $\mu \in L^1_{\text{loc}}([x_0, \bar{x}])$ and $\beta \in L^\infty([x_0, \bar{x}])$, for every $u_0 \in L^1([x_0, \bar{x}])$ the initial-boundary value problem defined by (A.1)–(A.2) and $u(0, \cdot) = u_0$ admits a unique solution $u(t, \cdot) \in L^1([x_0, \bar{x}])$ for $t \geq 0$. Moreover, the family of solution operators $\{T(t)\}_{t \geq 0}$, defined by $T(t)u_0 = u(t, \cdot)$, forms a strongly continuous and eventually compact semigroup of bounded linear operators in the Banach space $L^1([x_0, \bar{x}])$. Its IG $A: D(A) \rightarrow L^1([x_0, \bar{x}])$, defined as in (2.4), can be expressed as

$$A\phi = -\phi' - \mu\phi,$$

and its domain $D(A)$ can be characterized as

$$D(A) = \{\phi \in AC([x_0, \bar{x}]) \mid \mu\phi \in L^1([x_0, \bar{x}]), \phi(x_0) = K_\beta(\phi)\}.$$

Let us equip $AC([x_0, \bar{x}])$ with the norm $\|\cdot\|_{AC([x_0, \bar{x}])}$ defined as $\|f\|_{AC([x_0, \bar{x}])} := |f(x_0)| + \|f'\|_{L^1([x_0, \bar{x}])}$. Let $AC_0([x_0, \bar{x}])$ be the subspace of $AC([x_0, \bar{x}])$ of functions that are null at x_0 , which is a Banach space, being a closed subspace. The operator $V: L^1([x_0, \bar{x}]) \rightarrow AC_0([x_0, \bar{x}])$ defined by $V\phi(x) = \int_{x_0}^x \phi(\sigma) d\sigma$

defines an isomorphism between $L^1([x_0, \bar{x}])$ and $AC_0([x_0, \bar{x}])$, with $V^{-1}\psi = \psi'$ for all $\psi \in AC_0([x_0, \bar{x}])$. Observe that both V and V^{-1} are bounded ($\|V\| = \|V^{-1}\| = 1$).

We define the family of operators $\{S(t)\}_{t \geq 0}$ on $AC_0([x_0, \bar{x}])$ as $S(t) := VT(t)V^{-1}$. As in Section 3, we observe that they form a strongly continuous and eventually compact semigroup on $AC_0([x_0, \bar{x}])$ with IG $B: D(B) \rightarrow AC_0([x_0, \bar{x}])$, with $B := VAV^{-1}$ and $D(B) = VD(A)$. We can also derive the following expression for B , given $\psi \in D(B)$:

$$B\psi = -\psi' + K_\beta(\psi') - V(\mu\psi').$$

As in Section 3, we can conclude that A and B have the same spectrum, at most countable and consisting only of eigenvalues (of finite algebraic multiplicity).

As an example, let us choose $[x_0, \bar{x}] = [0, 2]$, $\mu(x) \equiv 1$ and $\beta(x) := e^{-x}$. It can be shown that the only real eigenvalue of the corresponding IG is the unique real solution of the equation

$$\frac{1 - e^{-2\lambda-4}}{\lambda + 2} = 1,$$

which can be approximated to the machine precision with standard methods (e.g., with MATLAB's `fzero` we obtain $\lambda = -1.203187869979980$). The relevant eigenfunction is

$$\phi(x) = e^{-\int_0^x \mu(s) ds - \lambda x} = e^{-(1+\lambda)x}.$$

We can observe in Figure 7 that the errors computed by our method decay with infinite order.

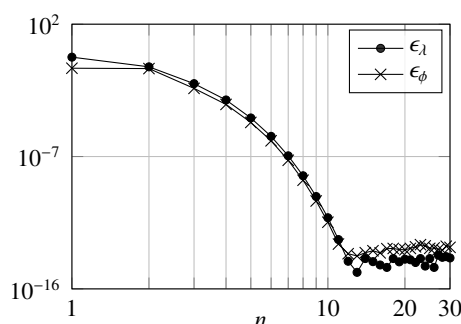


Figure 7. Errors ϵ_λ and ϵ_ϕ for the example of Appendix A.

Acknowledgments

We are grateful to Odo Diekmann for suggesting that we refer to the theory of absolute continuity in the sense of Carathéodory.

The authors are members of INdAM Research group GNCS. Davide Liessi and Francesca Scarabel are members of UMI Research group “Modellistica socio-epidemiologica”. The work of Simone De Reggi and Davide Liessi was supported by the Italian Ministry of University and Research (MUR) through the PRIN 2020 project (No. 2020JLWP23) “Integrated Mathematical Approaches to Socio-Epidemiological Dynamics” (CUP: E15F21005420006). Francesca Scarabel is supported by the UKRI

through the JUNIPER modelling consortium (grant number MR/V038613/1) and gratefully acknowledges the Dame Kathleen Ollerenshaw Trust and the London Mathematical Society for travel grants that facilitated the completion of this project.

Conflict of interest

The authors declare there is no conflict of interest.

References

1. F. Bekkal Brikci, J. Clairambault, B. Ribba, B. Perthame, An age-and-cyclin-structured cell population model for healthy and tumoral tissues, *J. Math. Biol.*, **57** (2008), 91–110. <https://doi.org/10.1007/s00285-007-0147-x>
2. J. Dyson, R. Villella-Bressan, G. Webb, A nonlinear age and maturity structured model of population dynamics, *J. Math. Anal. Appl.*, **242** (2000), 93–104. <https://doi.org/10.1006/jmaa.1999.6656>
3. K. E. Howard, A size and maturity structured model of cell dwarfism exhibiting chaotic behavior, *Internat. J. Bifur. Chaos Appl. Sci. Engrg.*, **13** (2003), 3001–3013. <https://doi.org/10.1142/S0218127403008363>
4. P. Magal, S. Ruan, *Structured Population Models in Biology and Epidemiology*, no. 1936 in Lecture Notes in Math., Springer, Berlin, Heidelberg, 2008. <https://doi.org/10.1007/978-3-540-78273-5>
5. J. A. J. Metz, O. Diekmann, *The Dynamics of Physiologically Structured Populations*, no. 68 in Lect. Notes Biomath., Springer, Berlin, Heidelberg, 1986. <https://doi.org/10.1007/978-3-662-13159-6>
6. H. Inaba, Endemic threshold analysis for the Kermack–McKendrick reinfection model, *Josai Math. Monogr.*, **9** (2016), 105–133. https://doi.org/10.20566/13447777_9_105
7. J. W. Sinko, W. Streifer, A new model for age-size structure of a population, *Ecology*, **48** (1967), 910–918. <https://doi.org/10.2307/1934533>
8. H. Kang, X. Huo, S. Ruan, On first-order hyperbolic partial differential equations with two internal variables modeling population dynamics of two physiological structures, *Ann. Mat. Pura Appl.*, **200** (2021), 403–452. <https://doi.org/10.1007/s10231-020-01001-5>
9. G. F. Webb, Dynamics of populations structured by internal variables, *Math. Z.*, **189** (1985), 319–335. <https://doi.org/10.1007/BF01164156>
10. D. Breda, O. Diekmann, M. Gyllenberg, F. Scarabel, R. Vermiglio, Pseudospectral discretization of nonlinear delay equations: New prospects for numerical bifurcation analysis, *SIAM J. Appl. Dyn. Syst.*, **15** (2016), 1–23. <https://doi.org/10.1137/15M1040931>
11. D. Breda, O. Diekmann, S. Maset, R. Vermiglio, A numerical approach for investigating the stability of equilibria for structured population models, *J. Biol. Dyn.*, **7** (2013), 4–20. <https://doi.org/10.1080/17513758.2013.789562>

12. D. Breda, P. Getto, J. Sánchez Sanz, R. Vermiglio, Computing the eigenvalues of realistic Daphnia models by pseudospectral methods, *SIAM J. Sci. Comput.*, **37** (2015), A2607–A2629. <https://doi.org/10.1137/15M1016710>
13. D. Breda, S. Maset, R. Vermiglio, Pseudospectral differencing methods for characteristic roots of delay differential equations, *SIAM J. Sci. Comput.*, **27** (2005), 482–495. <https://doi.org/10.1137/030601600>
14. D. Breda, C. Cusulin, M. Iannelli, S. Maset, R. Vermiglio, Stability analysis of age-structured population equations by pseudospectral differencing methods, *J. Math. Biol.*, **54** (2007), 701–720. <https://doi.org/10.1007/s00285-006-0064-4>
15. D. Breda, M. Iannelli, S. Maset, R. Vermiglio, Stability analysis of the Gurtin–MacCamy model, *SIAM J. Numer. Anal.*, **46** (2008), 980–995. <https://doi.org/10.1137/070685658>
16. F. Scarabel, D. Breda, O. Diekmann, M. Gyllenberg, R. Vermiglio, Numerical bifurcation analysis of physiologically structured population models via pseudospectral approximation, *Vietnam J. Math.*, **49** (2021), 37–67. <https://doi.org/10.1007/s10013-020-00421-3>
17. L. N. Trefethen, *Approximation Theory and Approximation Practice*, Society for Industrial and Applied Mathematics, Philadelphia, 2013.
18. D. Breda, S. Maset, R. Vermiglio, *Stability of Linear Delay Differential Equations*, SpringerBriefs Control Autom. Robot., Springer, New York, 2015. <https://doi.org/10.1007/978-1-4939-2107-2>
19. D. Breda, S. De Reggi, F. Scarabel, R. Vermiglio, J. Wu, Bivariate collocation for computing R_0 in epidemic models with two structures, *Comput. Math. Appl.*, **116**. <https://doi.org/10.1016/j.camwa.2021.10.026>
20. D. Breda, F. Florian, J. Ripoll, R. Vermiglio, Efficient numerical computation of the basic reproduction number for structured populations, *J. Comput. Appl. Math.*, **384** (2021), 113165. <https://doi.org/10.1016/j.cam.2020.113165>
21. D. Breda, T. Kuniya, J. Ripoll, R. Vermiglio, Collocation of next-generation operators for computing the basic reproduction number of structured populations, *J. Sci. Comput.*, **85** (2020), 40. <https://doi.org/10.1007/s10915-020-01339-1>
22. D. Breda, D. Liessi, Approximation of eigenvalues of evolution operators for linear renewal equations, *SIAM J. Numer. Anal.*, **56** (2018), 1456–1481. <https://doi.org/10.1137/17M1140534>
23. D. Breda, D. Liessi, Approximation of eigenvalues of evolution operators for linear coupled renewal and retarded functional differential equations, *Ric. Mat.*, **69** (2020), 457–481. <https://doi.org/10.1007/s11587-020-00513-9>
24. D. Breda, S. Maset, R. Vermiglio, Approximation of eigenvalues of evolution operators for linear retarded functional differential equations, *SIAM J. Numer. Anal.*, **50** (2012), 1456–1483. <https://doi.org/10.1137/100815505>
25. F. Scarabel, O. Diekmann, R. Vermiglio, Numerical bifurcation analysis of renewal equations via pseudospectral approximation, *J. Comput. Appl. Math.*, **397** (2021), 113611. <https://doi.org/10.1016/j.cam.2021.113611>
26. F. Scarabel, R. Vermiglio, Equations with infinite delay: Pseudospectral approximation of characteristic roots in an abstract framework, in preparation.

27. E. Sinestrari, G. F. Webb, Nonlinear hyperbolic systems with nonlocal boundary conditions, *J. Math. Anal. Appl.*, **121** (1987), 449–464. [https://doi.org/10.1016/0022-247X\(87\)90255-1](https://doi.org/10.1016/0022-247X(87)90255-1)
28. M. Iannelli, *Mathematical Theory of Age-Structured Population Dynamics*, Giardini Editori e Stampatori, Pisa, 1995.
29. H. Inaba, *Age-Structured Population Dynamics in Demography and Epidemiology*, Springer, Singapore, 2017. <https://doi.org/10.1007/978-981-10-0188-8>
30. P. P. J. E. Clément, H. J. A. M. Heijmans, S. Angenent, C. J. van Duijn, B. de Pagter, *One-Parameter Semigroups*, no. 5 in CWI Monogr., North-Holland Publishing Company, Netherlands, 1987.
31. K. J. Engel, R. Nagel, *One-Parameter Semigroups for Linear Evolution Equations*, no. 194 in Grad. Texts in Math., Springer, New York, 2000. <https://doi.org/10.1007/b97696>
32. O. Diekmann, S. A. van Gils, S. M. Verduyn Lunel, H.-O. Walther, *Delay Equations*, no. 110 in Appl. Math. Sci., Springer, New York, 1995. <https://doi.org/10.1007/978-1-4612-4206-2>
33. J. Šremr, Absolutely continuous functions of two variables in the sense of Carathéodory, *Electron. J. Differential Equations*, **2010** (2010), 154, 1–11.
34. L. N. Trefethen, *Spectral Methods in MATLAB*, Software Environ. Tools, Society for Industrial and Applied Mathematics, Philadelphia, 2000. <https://doi.org/10.1137/1.9780898719598>
35. J. P. Boyd, *Chebyshev and Fourier Spectral Methods*, 2nd edition, Dover, Mineola, NY, 2001, reprint of the Springer, Berlin, 1989 edition.
36. M. H. Schultz, L^∞ -multivariate approximation theory, *SIAM J. Numer. Anal.*, **6** (1969), 161–183. <https://doi.org/10.1137/0706017>
37. C. W. Clenshaw, A. R. Curtis, A method for numerical integration on an automatic computer, *SIAM J. Numer. Anal.*, **2** (1960), 197–205. <https://doi.org/10.1007/BF01386223>
38. L. N. Trefethen, Is Gauss quadrature better than Clenshaw–Curtis?, *SIAM Rev.*, **50** (2008), 67–87. <https://doi.org/10.1137/060659831>
39. A. M. de Roos, O. Diekmann, P. Getto, M. A. Kirkilionis, Numerical equilibrium analysis for structured consumer resource models, *Bull. Math. Biol.*, **72** (2010), 259–297. <https://doi.org/10.1007/s11538-009-9445-3>
40. C. Barril, À. Calsina, O. Diekmann, J. Z. Farkas, On the formulation of size-structured consumer resource models (with special attention for the principle of linearised stability), [arXiv:2111.09678](https://arxiv.org/abs/2111.09678).
41. À. Calsina, O. Diekmann, J. Z. Farkas, Structured populations with distributed recruitment: From PDE to delay formulation, *Math. Methods Appl. Sci.*, **39** (2016), 5175–5191. <https://doi.org/10.1002/mma.3898>
42. O. Diekmann, M. Gyllenberg, J. A. J. Metz, S. Nakaoka, A. M. de Roos, *Daphnia* revisited: Local stability and bifurcation theory for physiologically structured population models explained by way of an example, *J. Math. Biol.*, **61** (2010), 277–318. <https://doi.org/10.1007/s00285-009-0299-y>
43. E. Franco, O. Diekmann, M. Gyllenberg, Modelling physiologically structured populations: Renewal equations and partial differential equations, [arXiv:2201.05323](https://arxiv.org/abs/2201.05323).

44. E. Franco, M. Gyllenberg, O. Diekmann, One dimensional reduction of a renewal equation for a measure-valued function of time describing population dynamics, *Acta Appl. Math.*, **175** (2021), 12. <https://doi.org/10.1007/s10440-021-00440-3>
45. O. Diekmann, F. Scarabel, R. Vermiglio, Pseudospectral discretization of delay differential equations in sun-star formulation: Results and conjectures, *Discrete Contin. Dyn. Syst. Ser. S*, **13** (2020), 2575–2602. <https://doi.org/10.3934/dcdss.2020196>
46. M. Gyllenberg, F. Scarabel, R. Vermiglio, Equations with infinite delay: Numerical bifurcation analysis via pseudospectral discretization, *Appl. Math. Comput.*, **333** (2018), 490–505. <https://doi.org/10.1016/j.amc.2018.03.104>
47. G. F. Webb, *Theory of Nonlinear Age-Dependent Population Dynamics*, no. 89 in Monogr. Textb. Pure Appl. Math., Marcel Dekker, Inc., New York, 1985.



AIMS Press

© 2023 the Author(s), licensee AIMS Press. This is an open access article distributed under the terms of the Creative Commons Attribution License (<http://creativecommons.org/licenses/by/4.0>)